Longitudinal Active Suspension Control in a Half-Car Model with Unsprang Masses

Automatic Control
Electronic Engineering for Intelligent Vehicles
University of Bologna

A.A. 2025-2026

Alessandro Briccoli, Cristian Cecchini, Mario Di Marino

January 25, 2026

Abstract

This report presents the modeling, design, and simulation of an active suspension control system aimed at improving ride comfort and handling performance in passenger vehicles. The study focuses on a half-car model that includes both front and rear suspension dynamics, allowing the analysis of vertical and pitch motion of the vehicle body. Unlike passive suspension systems, which rely solely on spring-damper elements, the active suspension system introduced here incorporates actuators capable of generating controlled forces to counteract road disturbances in real time.

To achieve the desired ride quality, a control strategy based on Proportional-Integral-Derivative (PID) controllers is developed. Additionally, a state estimation technique using a Kalman observer is incorporated to provide real-time estimates of the states, helping to adapt to acceleration and road profile in a faster and more effective way.

The performance of the control system is evaluated through simulations conducted in MATLAB/Simulink. Results show a significant reduction in body acceleration and pitch angle variation when compared to a passive suspension system, demonstrating the effectiveness of the proposed approach in enhancing ride comfort. This project perfectly demonstrates, once again, the massive importance of active control strategies in automotive suspension design.

Chapter 1

Introduction

1.1 Motivations

Suspension systems play a crucial role in ensuring vehicle stability, comfort, and safety. Traditional passive suspensions cannot adapt to changing road conditions, leading to undesired oscillations and reduced performance.

In this project, focus on active suspension control in the longitudinal direction (front and rear), which aims to reduce vertical oscillations and pitch movements when the vehicle passes over bumps or uneven surfaces. The goal is to design a control system that keeps the car body as steady as possible, improving both passenger comfort and vehicle handling.

The half-car model was chosen because it provides a good trade-off between model simplicity and dynamic realism and allows to study the impact of front and rear suspension forces on the vehicle behavior without dealing with the complexity of a full 3D model.

1.2 List of the symbols

Table 1.1: Symbol Table

Symbol	Description	Dimension
x	State vector	$\mathbb{R}^n$
u	Control input vector	$\mathbb{R}^p$
y	Measured output vector	$\mathbb{R}^q$
e	Control error (goal)	$\mathbb{R}^{l_m}$
d	Disturbance vector	$\mathbb{R}^{l_d}$
r	Reference signal	$\mathbb{R}^{l_r}$
ν	Sensor noise	$\mathbb{R}^q$
w	Exogenous input, $w = \mathrm{col}(d, \nu, r)$	—
z	Vertical displacement of vehicle CoM	—
z_g	Vertical displacement of the road surface	—
θ	Vehicle pitch angle	—
$\dot{\theta}$	Angular velocity of pitch	—
θ_{gf}	Road pitch angle at front axle	—
ω_{gf}	Rate of change of front road pitch	—
θ_{gr}	Road pitch angle at rear axle	—
ω_{gr}	Rate of change of rear road pitch	—
x_i	Component of state vector x, $i = 1, \ldots, 8$	—
u_1	Vertical force component of actuator input	—
u_2	Pitch moment component of actuator input	—
f_{af}, f_{ar}	Forces from front and rear actuators	—
d_f, d_r	Distances from CoM to front and rear axles	—
f_2	Net vertical acceleration of vehicle body	—
f_4	Pitch angular acceleration	—
$\ddot{z}_g$	Vertical acceleration of road surface	—
α_{gf}, α_{gr}	Angular accelerations of road at front and rear axles	—
s_1, s_3	Suspension deflections (front, rear)	—
s_2, s_4	Suspension velocities (front, rear)	—
$f_s(p, v)$	Suspension force: $-kp - \beta v$	—
k	Suspension stiffness	—
β	Suspension damping coefficient	—
y_y, y_z	Lateral and vertical accelerometer readings	—
y_g	Gyroscope reading (pitch rate)	—
y_l, y_r	Suspension potentiometer readings (front, rear)	—
$\nu_y, \nu_z, \nu_g, \nu_l, \nu_r$	Sensor noise components	—
θ_a	Apparent pitch angle from accelerometers	—
r_z, r_θ	Reference vertical height and pitch angle	—
f_{sf}, f_{sr}	Suspension spring forces (front, rear)	—
f_{wf}, f_{wr}	Wheel forces (front, rear)	—
l_f, l_r	Lever arms of wheel forces for torque calculation	—
$E(y)$	Map from output to control error	—
g	Gravitational constant	—

1.2.1 Dynamic Model

The considered dynamic model represents a longitudinal half-car vehicle equipped with two active suspensions, accounting for both the vertical and pitch dynamics of the sprung mass, as well as the vertical motion of the unsprung masses at the front and rear axles. Unlike simplified rigid-body formulations, the inclusion of unsprung masses and tire stiffness enables the model to capture wheel–road interaction effects and high-frequency vertical dynamics, which are particularly relevant when road disturbances are present.

The system dynamics are described using a state vector composed of twelve states:

$$x = \begin{bmatrix} x_1 \\ x_2 \\ x_3 \\ x_4 \\ x_5 \\ x_6 \\ x_7 \\ x_8 \\ x_9 \\ x_{10} \\ x_{11} \\ x_{12} \end{bmatrix} = \begin{bmatrix} z_s \\ \dot{z}_s \\ \theta \\ \dot{\theta} \\ z_{wf} \\ \dot{z}_{wf} \\ z_{wr} \\ \dot{z}_{wr} \\ \theta_{gf} \\ \theta_{gr} \\ z_{gf} \\ z_{gr} \end{bmatrix} \tag{1.1}$$

The first four states describe the motion of the sprung mass: the vertical displacement and velocity of the vehicle body center of mass, together with the pitch angle and pitch rate. States z_{wf} and z_{wr}, along with their time derivatives, represent the vertical motion of the front and rear unsprung masses. Finally, the remaining states model the road excitation at the front and rear contact points in terms of vertical displacement and local pitch angle, allowing the road profile to be treated as an external disturbance.

The suspension system is actuated independently at the front and rear axles. For control purposes, the input vector is defined as:

$$u = \begin{bmatrix} u_1 \\ u_2 \end{bmatrix} = \begin{bmatrix} f_{af} + f_{ar} \\ f_{af} d_f - f_{ar} d_r \end{bmatrix} \tag{1.2}$$

where u_1 represents the resultant vertical force acting on the sprung mass, while u_2 corresponds to the pitching moment about the center of mass. This choice of inputs decouples the heave and pitch control objectives and simplifies the controller design.

The system dynamics are expressed in first-order nonlinear state-space form

as:

$$\dot{x} = \begin{bmatrix} x_2 \\ f_2 \\ x_4 \\ f_4 \\ x_6 \\ f_{wf} \\ x_8 \\ f_{wr} \\ \alpha_{gf} \\ \alpha_{gr} \\ \dot{z}_{gf} \\ \dot{z}_{gr} \end{bmatrix} \tag{1.3}$$

where f_2 and f_4 denote the vertical and pitch accelerations of the sprung mass, while f_{wf} and f_{wr} are the vertical accelerations of the front and rear unsprung masses, respectively. The quantities α_{gf} and α_{gr} represent the temporal variations of the road pitch profiles, and $\dot{z}_{gf}$ and $\dot{z}_{gr}$ describe the vertical velocities of the road surface at the wheel contact points.

The vertical acceleration of the sprung mass is obtained from Newton's second law as:

$$f_2 = -g + \frac{1}{m}\left(f_{sf} + f_{sr} + u_1\right) \tag{1.4}$$

where the gravitational acceleration acts downward, while the suspension forces and the control input contribute to the vertical force balance.

Similarly, the pitch angular acceleration about the vehicle center of mass is given by:

$$f_4 = \frac{1}{J}\left(d_f f_{sf} - d_r f_{sr} + u_2\right) \tag{1.5}$$

which expresses the balance of moments generated by the front and rear suspension forces and the control-induced pitching moment.

The suspension deflections and relative velocities are defined as:

$$s_1 = (z_s - z_{wf}) + d_f(\theta - \theta_{gf}), \qquad s_3 = (z_s - z_{wr}) - d_r(\theta + \theta_{gr}) \tag{1.6}$$

$$s_2 = (\dot{z}_s - \dot{z}_{wf}) + d_f(\dot{\theta} - \dot{\theta}_{gf}), \qquad s_4 = (\dot{z}_s - \dot{z}_{wr}) - d_r(\dot{\theta} - \dot{\theta}_{gr}) \tag{1.7}$$

These expressions account for both the translational and rotational motion of the sprung mass relative to the unsprung masses, including the effect of road pitch disturbances.

The suspension forces are modeled as linear spring-damper elements:

$$f_{sf} = -ks_1 - \beta s_2, \qquad f_{sr} = -ks_3 - \beta s_4 \tag{1.8}$$

where k and β denote the suspension stiffness and damping coefficients, respectively.

The tire–road interaction is modeled using linear tire stiffness:

$$f_{tf} = k_{tf}(z_{gf} - z_{wf}), \qquad f_{tr} = k_{tr}(z_{gr} - z_{wr}) \tag{1.9}$$

which relates the tire forces to the relative displacement between the road surface and the unsprung masses.

The dynamics of the unsprung masses are governed by:

$$f_{wf} = \frac{1}{m_{wf}} \left(f_{tf} - f_{sf} - f_{af} - m_{wf} g\right) \tag{1.10}$$

$$f_{wr} = \frac{1}{m_{wr}} \left(f_{tr} - f_{sr} - f_{ar} - m_{wr} g\right) \tag{1.11}$$

where each unsprung mass is subjected to the tire force, suspension force, actuator force, and gravity.

Finally, the actuator forces applied at the front and rear suspensions are recovered from the control inputs as:

$$f_{af} = \frac{d_r u_1 + u_2}{d_f + d_r}, \tag{1.12}$$

$$f_{ar} = \frac{d_f u_1 - u_2}{d_f + d_r} \tag{1.13}$$

This formulation provides a complete nonlinear state-space description of the half-car dynamics, explicitly capturing the coupled behavior of the vehicle body, suspensions, unsprung masses, and road disturbances.

1.2.2 Sensor Model

The effectiveness of the control architecture relies heavily on the accurate and timely acquisition of physical quantities related to the vehicle's motion and posture. To this end, the half-car system is equipped with a set of onboard sensors, specifically selected to ensure observability of the dynamic model and to allow real-time feedback control.

Measurement Vector The complete sensor output is gathered in the measurement vector:

$$y = \begin{bmatrix} y_y \\ y_z \\ y_g \\ y_l \\ y_r \end{bmatrix} = \begin{bmatrix} \sin x_3 (f_2 + g) + \cos x_3 (f_{wr} + f_{wf})/m \\ \cos x_3 (f_2 + g) - \sin x_3 (f_{wr} + f_{wf})/m \\ x_4 \\ s_1 \\ s_3 \end{bmatrix} + \nu \tag{1.14}$$

This vector includes measurements from two accelerometers, one gyroscope, and two linear potentiometers, all subject to additive noise ν.

Accelerometers The first two components y_y and y_z represent the lateral and vertical accelerations measured in the vehicle's body-fixed reference frame. These measurements are obtained via two MEMS accelerometers mounted at the vehicle's center of mass. Due to the non-inertial frame of reference, the accelerations are nonlinear combinations of translational and rotational dynamics and include the gravitational component projected along the vehicle's pitch angle $x_3 = \theta$.

These measurements are used to estimate the apparent pitch angle θ_a, which is a key feedback signal for pitch stabilization control. We assume a typical sensor such as the **STMicroelectronics LIS3DH**, offering 12-bit resolution, low noise density ($\sim 50\ \mu g/\sqrt{Hz}$), and a digital output interface.

Figure 1.1: STM LIS3DH Sensor used as accelerometer

Gyroscope. The third component y_g corresponds to the pitch angular rate $\dot{\theta}$, measured directly by a gyroscope mounted on the vehicle frame. This measurement provides high-frequency information essential for dynamic feedback control and stability monitoring.

A typical device used could be the **Bosch BMI160** inertial measurement unit (IMU), with integrated accelerometer and gyroscope, capable of delivering low-latency angular rate data with high sensitivity (16-bit ADC) and low drift. The sensor is assumed to be rigidly fixed to the main chassis near the center of rotation to minimize errors due to offset and vibration.

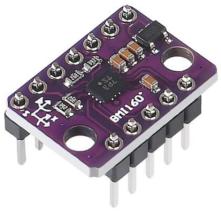

Figure 1.2: Bosch BMI160 soldered in a circuit used as a gyroscope

Suspension Potentiometers. The fourth and fifth entries y_l and y_r are deflection measurements of the front and rear suspension struts, modeled by the quantities s_1 and s_3. These values are acquired via linear position sensors (e.g., **SLS190**) mounted along the suspension path to detect extension or compression relative to the static rest position.

These readings give direct insight into the interaction between the vehicle and the road surface, reflecting terrain irregularities, road disturbances, and load shifts. Additionally, they are fundamental to compute control actions that regulate ride comfort and load distribution.

Figure 1.3: Linear Potentiometer SLS190

Noise Modeling All sensor measurements are corrupted by additive noise:

$$\nu = \begin{bmatrix} \nu_y & \nu_z & \nu_g & \nu_l & \nu_r \end{bmatrix}^T$$

A Gaussian-distributed noise is assumed with known standard deviations derived from the sensor datasheets. Noise in the accelerometers and gyroscope may include both white noise and low-frequency bias drift, while potentiometers may exhibit quantization and thermal noise. These uncertainties justify the implementation of robust filtering (e.g., Kalman filters) and noise-resilient control laws.

Sensor Placement and Observability The sensor configuration is designed to ensure full observability of the system state vector x required for control. The accelerometers and gyroscope reconstruct the translational and rotational dynamics, while the suspension sensors resolve wheel-body interactions. This sensor suite has been tested in simulation to confirm that it enables estimation of all states through standard observers.

Practical Considerations While alternative sensors such as LIDAR, GPS, or magnetometers could enhance localization in other contexts, they are not considered here due to their inadequacy in indoor or suspension-focused scenarios. For example, GPS is unsuitable for fine-grained control of vertical dynamics or in indoor testing environments, and magnetometers are highly susceptible to interference from ferromagnetic chassis components and electromagnetic noise from motors.

The selected sensor set offers a balance between cost, precision, and real-time capability, making it well-suited for embedded automotive platforms focused on suspension control and ride dynamics.

Control Objectives We define the apparent pitch angle θ_a using accelerometer data:

$$\theta_a = \sin^{-1}\left(\frac{y_y}{\sqrt{y_y^2 + y_z^2}}\right) \tag{1.15}$$

The control error vector is defined as:

$$e = \begin{bmatrix} \frac{y_f d_r + y_r d_f}{d_r + d_f} - r_z \\ \theta_a - r_\theta \end{bmatrix} \tag{1.16}$$

This error describes deviations from the desired vertical height and perceived pitch. The control task is to design u to drive $e \to 0$ in the presence of disturbances and noise.

The second component of the error vector $he(x, u, w)$ captures the deviation from a desired apparent pitch angle θ_a, which reflects the passenger-perceived acceleration. It is defined through the nonlinear relationship:

$$\sin(\theta_a) = \frac{y_y}{\sqrt{y_y^2 + y_z^2}} \quad \Rightarrow \quad \theta_a = \sin^{-1}\left(\frac{y_y}{\sqrt{y_y^2 + y_z^2}}\right) \tag{1.17}$$

where y_y and y_z are the accelerometer outputs along the body-frame y and z axes, respectively. This formulation provides an estimate of the pitch experienced by passengers during acceleration, braking, or uneven ground contact.

The complete output error function thus becomes:

$$he(x, u, w) = \begin{bmatrix} \dfrac{(s_1 + \nu_f)d_r + (s_3 + \nu_r)d_f}{d_r + d_f} - r_z \\ \sin^{-1}\left(\dfrac{h_1 + \nu_y}{\sqrt{(h_1 + \nu_y)^2 + (h_2 + \nu_z)^2}}\right) - r_\theta \end{bmatrix} \tag{1.18}$$

where s_1, s_3 are suspension deflections, h_1, h_2 are derived from dynamic equations, and ν_i are sensor noise terms. This formulation ensures the controller minimizes both height and perceptual pitch deviations.

1.2.3 System Linearization

To facilitate the control design of the longitudinal half-car model equipped with active front and rear suspension systems, the initial step involves the linearization of the nonlinear system dynamics. This process is performed by identifying appropriate steady-state operating points (x^*, y^*, w^*), which characterize representative conditions under which the vehicle is expected to operate. Linearizing the system around these equilibrium points enables the derivation of a time-invariant linear approximation of the vehicle dynamics, thereby simplifying the synthesis and analysis of control strategies.

Linearization Around the Operating Point

Consider the nonlinear system model:

$$\begin{aligned} \dot{x} &= f(x, u, w), \quad x(t_0) = x_0 \\ y &= h(x, u, w) \\ e &= h_e(x, u, w) \end{aligned} \tag{1.19}$$

The steady-state operating points $(x^\star, u^\star, w^\star)$ is called *equilibrium triplet* if satisfies the condition:

$$f(x^\star, u^\star, w^\star) = 0 \tag{1.20}$$

and defines the equilibrium output and error as:

$$y^\star := h(x^\star, u^\star, w^\star), \quad e^\star := h_e(x^\star, u^\star, w^\star) \tag{1.21}$$

The variations around the equilibrium point are defined as:

$$\begin{aligned}\tilde{x} &:= x - x^\star \\ \tilde{y} &:= y - y^\star \\ \tilde{e} &:= e - e^\star \\ \tilde{u} &:= u - u^\star \\ \tilde{w} &:= w - w^\star\end{aligned} \tag{1.22}$$

Using the fact that $\dot{x}^\star = 0$, the dynamics of the variations are:

$$\begin{aligned}\dot{\tilde{x}} &= f(x^\star + \tilde{x}, u^\star + \tilde{u}, w^\star + \tilde{w}), \quad \tilde{x}(t_0) = x_0 - x^\star \\ \tilde{y} &= h(x^\star + \tilde{x}, u^\star + \tilde{u}, w^\star + \tilde{w}) \\ \tilde{e} &= h_e(x^\star + \tilde{x}, u^\star + \tilde{u}, w^\star + \tilde{w})\end{aligned} \tag{1.23}$$

To obtain a tractable model for controller synthesis, a first-order Taylor expansion is applied around the equilibrium point. The resulting Jacobian matrices are defined as:

$$\begin{aligned}A &:= \left.\frac{\partial f(x,u,w)}{\partial x}\right|_{\substack{x=x^\star \\ u=u^\star \\ w=w^\star}} & B_1 &:= \left.\frac{\partial f(x,u,w)}{\partial u}\right|_{\substack{x=x^\star \\ u=u^\star \\ w=w^\star}} & B_2 &:= \left.\frac{\partial f(x,u,w)}{\partial w}\right|_{\substack{x=x^\star \\ u=u^\star \\ w=w^\star}} \\ C &:= \left.\frac{\partial h(x,u,w)}{\partial x}\right|_{\substack{x=x^\star \\ u=u^\star \\ w=w^\star}} & D_1 &:= \left.\frac{\partial h(x,u,w)}{\partial u}\right|_{\substack{x=x^\star \\ u=u^\star \\ w=w^\star}} & D_2 &:= \left.\frac{\partial h(x,u,w)}{\partial w}\right|_{\substack{x=x^\star \\ u=u^\star \\ w=w^\star}} \\ C_e &:= \left.\frac{\partial h_e(x,u,w)}{\partial x}\right|_{\substack{x=x^\star \\ u=u^\star \\ w=w^\star}} & D_{e1} &:= \left.\frac{\partial h_e(x,u,w)}{\partial u}\right|_{\substack{x=x^\star \\ u=u^\star \\ w=w^\star}} & D_{e2} &:= \left.\frac{\partial h_e(x,u,w)}{\partial w}\right|_{\substack{x=x^\star \\ u=u^\star \\ w=w^\star}}\end{aligned} \tag{1.24}$$

Neglecting second-order terms, the linearized system becomes the so-called *design model*:

$$\begin{cases}\dot{\tilde{x}} = A\tilde{x} + B_1\tilde{u} + B_2\tilde{w}, \quad \tilde{x}(t_0) = x_0 - x^\star \\ \tilde{y} = C\tilde{x} + D_1\tilde{u} + D_2\tilde{w} \\ \tilde{e} = C_e\tilde{x} + D_{e1}\tilde{u} + D_{e2}\tilde{w}\end{cases} \tag{1.25}$$

This Linear Time-Invariant (LTI) approximation of the nonlinear model is valid in a neighborhood of the equilibrium point, enabling efficient analysis and controller design under small perturbations.

Matrix calculus todo: ricalcolare For the matrix calculation, the procedure described in equations (1.24) was followed. By substituting the equilibrium triplet given in (1.20), obtaining the following matrices:

$$A = \begin{bmatrix} 0 & 1 & 0 & 0 & 0 & 0 & 0 & 0 \\ -\frac{2k}{m} & -\frac{2\beta}{m} & -\frac{d_f k - d_r k}{m} & -\frac{\beta d_f - \beta d_r}{m} & \frac{d_f k}{m} & -\frac{d_r k}{m} & \frac{\beta d_f}{m} & -\frac{\beta d_r}{m} \\ 0 & 0 & 0 & 1 & 0 & 0 & 0 & 0 \\ -\frac{d_f k - d_r k}{J} & -\frac{\beta d_f - \beta d_r}{J} & -\frac{k d_f^2 + k d_r^2}{J} & -\frac{\beta d_f^2 + \beta d_r^2}{J} & \frac{k d_f^2}{J} & \frac{k d_r^2}{J} & \frac{\beta d_f^2}{J} & \frac{\beta d_r^2}{J} \\ 0 & 0 & 0 & 0 & 1 & 0 & 0 & 0 \\ 0 & 0 & 0 & 0 & 0 & 1 & 0 & 0 \\ 0 & 0 & 0 & 0 & 0 & 0 & 0 & 0 \\ 0 & 0 & 0 & 0 & 0 & 0 & 0 & 0 \end{bmatrix} \tag{1.26}$$

$$B_1 = \begin{bmatrix} 0 & 0 \\ \frac{1}{m} & 0 \\ 0 & 0 \\ 0 & \frac{1}{J} \\ 0 & 0 \\ 0 & 0 \\ 0 & 0 \\ 0 & 0 \end{bmatrix} \tag{1.27}$$

$$B_2 = \begin{bmatrix} 0 & 0 & 0 & 0 & 0 \\ -1 & 0 & 0 & 0 & 0 \\ 0 & 0 & 0 & 0 & 0 \\ 0 & 0 & 0 & \frac{\ell_0 + \Delta_0}{J} & \frac{\ell_0 + \Delta_0}{J} \\ 0 & 0 & 0 & 0 & 0 \\ 0 & 0 & 0 & 0 & 0 \\ 0 & 1 & 0 & 0 & 0 \\ 0 & 0 & 1 & 0 & 0 \end{bmatrix} \tag{1.28}$$

$$C = \begin{bmatrix} 0 & 0 & g & 0 & 0 & 0 & 0 & 0 \\ -\frac{2k}{m} & -\frac{2\beta}{m} & -\frac{(d_f k - d_r k)}{m} & -\frac{(\beta d_f - \beta d_r)}{m} & \frac{d_f k}{m} & -\frac{d_r k}{m} & \frac{\beta d_f}{m} & -\frac{\beta d_r}{m} \\ 0 & 0 & 0 & 1 & 0 & 0 & 0 & 0 \\ 1 & 0 & d_f & 0 & -d_f & 0 & 0 & 0 \\ 1 & 0 & -d_r & 0 & 0 & d_r & 0 & 0 \end{bmatrix} \tag{1.29}$$

$$D_1 = \begin{bmatrix} 0 & 0 \\ \frac{1}{m} & 0 \\ 0 & 0 \\ 0 & 0 \\ 0 & 0 \end{bmatrix} \tag{1.30}$$

$$D_2 = \begin{bmatrix} 0 & 0 & 0 & \frac{1}{m} & \frac{1}{m} & 1 & 0 & 0 & 0 & 0 & 0 & 0 \\ 0 & 0 & 0 & 0 & 0 & 0 & 1 & 0 & 0 & 0 & 0 & 0 \\ 0 & 0 & 0 & 0 & 0 & 0 & 0 & 1 & 0 & 0 & 0 & 0 \\ 0 & 0 & 0 & 0 & 0 & 0 & 0 & 0 & 1 & 0 & 0 & 0 \\ 0 & 0 & 0 & 0 & 0 & 0 & 0 & 0 & 0 & 1 & 0 & 0 \end{bmatrix} \tag{1.31}$$

$$C_e = \begin{bmatrix} 1 & 0 & 0 & 0 & -\frac{d_f d_r}{d_f + d_r} & \frac{d_f d_r}{d_f + d_r} & 0 & 0 \\ 0 & 0 & 1 & 0 & 0 & 0 & 0 & 0 \end{bmatrix} \tag{1.32}$$

$$\mathrm{D_{e1}} = \begin{bmatrix} 0 & 0 \\ 0 & 0 \end{bmatrix} \tag{1.33}$$

$$D_{e2} \begin{bmatrix} 0 & 0 & 0 & 0 & 0 & 0 & 0 & 0 & \frac{d_r}{d_f + d_r} & \frac{d_f}{d_f + d_r} & -1 & 0 \\ 0 & 0 & 0 & \frac{1}{mg} & \frac{1}{mg} & \frac{1}{g} & 0 & 0 & 0 & 0 & 0 & -1 \end{bmatrix} \tag{1.34}$$

Numerical Matrices To calculate the numerical values of the matrices, the parameters were replaced with the values of the vehicle chosen for this study: All parameters used to find the numeric matrices are based on the Tesla Model S, a car suitable for this type of active suspensions and with same suspension paramethers on front and rear axle, this simplifies slighlty our model:

Simbolo	**Descrizione**	**Valore**	**Unità**
m	Total mass of the car	1085	kg
k	Suspension stiffness	30000	N/m
β	Estimated damping coefficient	2000	N/(m/s)
ℓ_0	Suspension height at rest	0.5	m
g	Gravitational force	9.81	m/s^2
d_f	Front axle distance from CoM	1.362	m
d_r	Rear axle distance from CoM	1.598	m
J	Pitch moment of inertia	4870	$kg \cdot m^2$

Table 1.2: Dynamic model parameters of a Tesla Model S

Figure 1.4: Tesla Model S

$$A = \begin{bmatrix} 0 & 1 & 0 & 0 & 0 & 0 & 0 & 0 \\ -55.2995 & -3.68664 & 6.52535 & 0.435023 & 37.659 & -44.1843 & 2.5106 & -2.94562 \\ 0 & 0 & 0 & 1 & 0 & 0 & 0 & 0 \\ 1.4538 & 0.0969199 & -27.158 & -1.81053 & 11.4274 & 15.7306 & 0.761825 & 1.04871 \\ 0 & 0 & 0 & 0 & 1 & 0 & 0 & 0 \\ 0 & 0 & 0 & 0 & 0 & 1 & 0 & 0 \\ 0 & 0 & 0 & 0 & 0 & 0 & 0 & 0 \\ 0 & 0 & 0 & 0 & 0 & 0 & 0 & 0 \end{bmatrix}$$

$$B_1 = \begin{bmatrix} 0 & 0 \\ 0.000921659 & 0 \\ 0 & 0 \\ 0 & 0.000205339 \\ 0 & 0 \\ 0 & 0 \\ 0 & 0 \\ 0 & 0 \end{bmatrix} \quad B_2 = \begin{bmatrix} 0 & 0 & 0 & 0 & 0 \\ -1 & 0 & 0 & 0 & 0 \\ 0 & 0 & 0 & 0 & 0 \\ 0 & 0 & 0 & 0.0000662428 & 0.0000662428 \\ 0 & 0 & 0 & 0 & 0 \\ 0 & 0 & 0 & 0 & 0 \\ 0 & 1 & 0 & 0 & 0 \\ 0 & 0 & 1 & 0 & 0 \end{bmatrix}$$

$$C = \begin{bmatrix} 0 & 0 & 9.81 & 0 & 0 & 0 & 0 & 0 \\ -55.2995 & -3.68664 & 6.52535 & 0.435023 & 37.659 & -44.1843 & 2.5106 & -2.94562 \\ 0 & 0 & 0 & 1 & 0 & 0 & 0 & 0 \\ 1 & 0 & 1.362 & 0 & -1.362 & 0 & 0 & 0 \\ 1 & 0 & -1.598 & 0 & 0 & 1.598 & 0 & 0 \end{bmatrix}$$

$$D_1 = \begin{bmatrix} 0 & 0 \\ 0.000921659 & 0 \\ 0 & 0 \\ 0 & 0 \\ 0 & 0 \end{bmatrix} \quad D_2 = \begin{bmatrix} 0 & 0 & 0 & 0.000921659 & 0.000921659 & 1 & 0 & 0 & 0 & 0 & 0 & 0 \\ 0 & 0 & 0 & 0 & 0 & 0 & 1 & 0 & 0 & 0 & 0 & 0 \\ 0 & 0 & 0 & 0 & 0 & 0 & 0 & 1 & 0 & 0 & 0 & 0 \\ 0 & 0 & 0 & 0 & 0 & 0 & 0 & 0 & 1 & 0 & 0 & 0 \\ 0 & 0 & 0 & 0 & 0 & 0 & 0 & 0 & 0 & 1 & 0 & 0 \end{bmatrix}$$

$$C_e = \begin{bmatrix} 1 & 0 & 0 & 0 & -0.735296 & 0.735296 & 0 & 0 \\ 0 & 0 & 1 & 0 & 0 & 0 & 0 & 0 \end{bmatrix}$$

$$D_{e2} = \begin{bmatrix} 0 & 0 & 0 & 0 & 0 & 0 & 0 & 0 & 0.539865 & 0.460135 & -1 & 0 \\ 0 & 0 & 0 & 0.000093951 & 0.000093951 & 0.101937 & 0 & 0 & 0 & 0 & 0 & -1 \end{bmatrix}$$

1.2.4 Linear Model Analysis

To support the development of an effective suspension controller and gain insight into the vehicle's dynamic behavior, we examine a linearized model of a half-car system. This analysis is performed around a nominal equilibrium point, where the vehicle is at rest with zero pitch angle and no vertical or angular velocities. The focus is on the open-loop dynamics of the vehicle body, excluding actuator behavior and wheel compliance.

The model captures the essential vertical (heave) and angular (pitch) motions of the chassis. The state vector is defined as:

$$x = \begin{bmatrix} z - z_0 \\ \dot{z} \\ \theta \\ \dot{\theta} \end{bmatrix} \tag{1.35}$$

where z_0 is the vertical position of the center of mass at static equilibrium, and θ denotes the pitch angle of the chassis. The state-space representation of the system is given by:

$$\dot{x} = A_{\text{int}} x \tag{1.36}$$

Analysis of this reduced 4x4 matrix will be performed, ignoring the 4 exogenous states, the reason behind this is explained later in chapter 1.3 (Reachability) **todo: ricalcolare**

$$A_{\text{int}} = \begin{bmatrix} 0 & 1 & 0 & 0 \\ -55.2995 & -3.68664 & 6.52535 & 0.435023 \\ 0 & 0 & 0 & 1 \\ 1.4538 & 0.0969199 & -27.158 & -1.81053 \end{bmatrix} \tag{1.37}$$

This matrix characterizes the coupled dynamics of the system, with off-diagonal elements indicating interaction between vertical and angular motions. Such coupling arises naturally in a physical half-car system, where vertical displacements can induce pitching, and vice versa.

1.2.5 Open-Loop Dynamics

To evaluate the system's stability and transient behavior, is necessary to calculate the eigenvalues of the matrix A_{int} by solving the characteristic equation:

$$\det(A_{\text{int}} - \lambda I) = 0 \tag{1.38}$$

The resulting eigenvalues are:

todo: ricalcolare

$$\lambda_{1,2} = -1.55 \pm j6.28, \quad \lambda_{3,4} = -2.47 \pm j5.10 \tag{1.39}$$

The eigenvalues form two pairs of complex conjugates, each with negative real parts, indicating that the system is asymptotically stable in open loop. These pairs represent distinct oscillatory modes characterized by different damping and frequency properties:

- The eigenvalues $\lambda_{1,2}$ correspond to a lightly damped oscillatory mode with a higher frequency.
- The eigenvalues $\lambda_{3,4}$ correspond to a more heavily damped mode with a lower oscillation frequency.

Due to the coupling present in A_{int}, these modes represent mixed heave-pitch dynamics rather than purely vertical or angular motions. This hybrid behavior implies that any disturbance in one degree of freedom can propagate to the other, necessitating a control strategy that accounts for this interaction.

The system's open-loop stability ensures that disturbances decay over time, but the oscillatory nature of the transients may degrade ride comfort and vehicle handling. Therefore, active suspension control is warranted to suppress these vibrations more rapidly, reduce settling time, and improve overall vehicle performance.

In summary, the linearized model described by A_{int} reveals a stable but dynamically coupled system with oscillatory characteristics. These insights are essential for the design of coordinated control strategies that enhance both ride quality and dynamic response.

1.3 Control

Reachability

In this section, a reachability analysis is carried out to determine which parts of the system's state space can be influenced by the control input. Starting from the linearized state-space system:

$$\dot{\tilde{x}} = A\tilde{x} + B_1\tilde{u} \tag{1.40}$$

we aim to identify which states can be driven from the origin to a desired position through the control input $\tilde{u}$. The reachability matrix is defined as:

$$\mathcal{R} = \begin{bmatrix} B_1 & AB_1 & A^2B_1 & \dots & A^{n-1}B_1 \end{bmatrix} \tag{1.41}$$

A linear time-invariant system is said to be **fully reachable** (or controllable from the origin) if the rank of $\mathcal{R}$ is equal to n, the number of state variables. In such a case, it is possible to design a state feedback controller that places all eigenvalues of the closed-loop system arbitrarily.

In our case, the system has $n = 8$ state variables. These include both the vehicle body dynamics (vertical position and velocity, pitch angle and rate) and road-related exogenous components (front and rear road pitch angles and their derivatives). The control input $\tilde{u} \in \mathbb{R}^2$ acts through actuators located at the front and rear suspensions, influencing primarily the body dynamics of the vehicle.

However, the states related to the road excitation are not directly controllable. As such, only a subset of the full state vector can be affected by $\tilde{u}$. Upon computation of the reachability matrix $\mathcal{R}$ using the specific system matrices A and B_1, we obtain:
todo: ricalcolare

```
R = ctrb(A, B1);
rank_R = rank(R);
```

$$\text{rank}(\mathcal{R}) = 4 < 8 \tag{1.42}$$

This indicates that the system is **not fully reachable**. Only the four states corresponding to the internal dynamics of the vehicle body are reachable, while the remaining four states — associated with the road profile — are uncontrollable and must be treated as external disturbances. Consequently, control strategies such as state feedback and optimal control (e.g., LQR) can only be designed for the reachable subspace.

Reduced Reachability Analysis In the present model, the state vector $\tilde{x} \in \mathbb{R}^8$ includes eight components. However, the last four states represent environmental or road-related variables (e.g., road profile curvature), which evolve independently of the control input $\tilde{u}$. These are known as **exogenous states** and are not directly controllable.

Therefore, reachability analysis is performed only on the first four states, which represent the internal vehicle dynamics and are influenced by control inputs. Let A_{int} and $B_{1,\text{int}}$ be the upper-left 4×4 and 4×2 blocks of matrices A and B_1:

todo: ricalcolare

$$A_{\text{int}} = \begin{bmatrix} 0 & 1 & 0 & 0 \\ -55.2995 & -3.68664 & 6.52535 & 0.435023 \\ 0 & 0 & 0 & 1 \\ 1.4538 & 0.0969199 & -27.158 & -1.81053 \end{bmatrix} \tag{1.43}$$

$$B_{1,\text{int}} = \begin{bmatrix} 0 & 0 \\ 0.000921659 & 0 \\ 0 & 0 \\ 0 & 0.000205339 \end{bmatrix} \tag{1.44}$$

$$\dot{\tilde{x}}_{\text{int}} = A_{\text{int}} \tilde{x}_{\text{int}} + B_{1,\text{int}} \tilde{u} \tag{1.45}$$

The reachability matrix becomes:

$$\mathcal{R}_{\text{int}} = \begin{bmatrix} B_{1,\text{int}} & A_{\text{int}} B_{1,\text{int}} & A_{\text{int}}^2 B_{1,\text{int}} & A_{\text{int}}^3 B_{1,\text{int}} \end{bmatrix} \tag{1.46}$$

An evaluation of the rank of this matrix using MATLAB's `ctrb` function:

```
R_int = ctrb(A_int, B1_int);
rank(R_int)
```

The resulting rank is 4, which confirms that the internal subsystem is fully reachable.

Stabilizability and the Hurwitz Condition According to control theory, if the system is fully reachable, it is possible to design a state feedback control law:

$$\tilde{u} = K_S \tilde{x}_{\text{int}} \tag{1.47}$$

such that the closed-loop matrix:

$$A_{\text{int}} + B_{1,\text{int}} K_S \tag{1.48}$$

is **Hurwitz**, meaning that all of its eigenvalues lie in the left half of the complex plane. This ensures that the closed-loop system is **BIBS stable** (Bounded

Input Bounded State): all state trajectories remain bounded in response to bounded inputs.

In conclusion, while the full model is not entirely reachable due to the presence of exogenous states, the subsystem representing the vehicle dynamics is fully reachable and can be stabilized using linear state feedback.

Integral Action

While the stabilizer matrix K_S ensures the stability of the internal system under feedback control, an integral action is required to eliminate steady-state error in the presence of unknown constant disturbances $\tilde{w}$.

The regulated error $\tilde{e}$ is defined as:

$$\tilde{e} = C_e\tilde{x} + D_{1e}\tilde{u} + D_{2e}\tilde{w} \tag{1.49}$$

To implement integral control, new integral state η is introduced:

$$\dot{\eta} = \tilde{e} \tag{1.50}$$

This leads to an extended state vector:

$$x_e = \begin{bmatrix} \tilde{x} \\ \eta \end{bmatrix} \tag{1.51}$$

The extended system dynamics are:

$$\dot{x}_e = \bar{A}x_e + \bar{B}_1\tilde{u} + \bar{B}_2\tilde{w} \tag{1.52}$$

where

$$\bar{A} = \begin{bmatrix} A & 0 \\ C_e & 0 \end{bmatrix}, \quad \bar{B}_1 = \begin{bmatrix} B_1 \\ D_{1e} \end{bmatrix}, \quad \bar{B}_2 = \begin{bmatrix} B_2 \\ D_{2e} \end{bmatrix} \tag{1.53}$$

To verify whether the extended system is controllable (reachable), a reachability matrix is computed as:

$$\mathcal{R}_e = \begin{bmatrix} \bar{B}_1 & \bar{A}\bar{B}_1 & \bar{A}^2\bar{B}_1 & \cdots & \bar{A}^{n+q-1}\bar{B}_1 \end{bmatrix} \tag{1.54}$$

where n is the number of original state variables and q is the number of integrator states. In this model, $n = 4$ (excluding the four uncontrollable states) and $q = 2$, so we expect:

$$\text{rank}(\mathcal{R}_e) = 6 \tag{1.55}$$

The reachability matrix is constructed in MATLAB using:

```
Ae = [A, zeros(6,2); Ce, zeros(2,2)];
B1e = [B1; D1e];
Re = ctrb(Ae, B1e);
rank(Re)
```

Result: The output of the command confirms that $\text{rank}(\mathcal{R}_e) = 6$, i.e., the extended system is fully reachable.

Conclusion: Since the extended system is reachable, it is possible to design a state feedback control law of the form:

$$\tilde{u} = \bar{K}x_e = K_S\tilde{x} + K_I\eta \tag{1.56}$$

such that the closed-loop matrix $\bar{A} + \bar{B}_1\bar{K}$ is Hurwitz. This guarantees asymptotic stability of the augmented system and drives the regulation error $\tilde{e}$ to zero.

Observability

Up to this point, the system state $\tilde{x}$ has been assumed to be known. However, this assumption is often unrealistic, particularly when some state variables are not directly measurable. For this reason, a state observer is required to estimate the internal states based on measurable outputs.

Given that the last four states of $\tilde{x}$ are exogenous and not influenced by the system dynamics, we restrict our observability analysis to the internal dynamics only, i.e., $\tilde{x}_{\text{int}} \in \mathbb{R}^4$.

Let C_{int} be the output matrix corresponding to the internal states. Then, the observability matrix is given by:

todo: ricalcolare

$$\mathcal{O} = \begin{bmatrix} C_{\text{int}} \\ C_{\text{int}}A_{\text{int}} \\ C_{\text{int}}A_{\text{int}}^2 \\ C_{\text{int}}A_{\text{int}}^3 \end{bmatrix} \tag{1.57}$$

$$C_{\text{int}} = \begin{bmatrix} 0 & 0 & 9.81 & 0 \\ -55.2995 & -3.68664 & 6.52535 & 0.435023 \\ 0 & 0 & 0 & 1 \\ 1 & 0 & 1.362 & 0 \\ 1 & 0 & -1.598 & 0 \\ 0 & 0 & 0 & 0 \\ 0 & 0 & 0 & 0 \end{bmatrix} \tag{1.58}$$

Using MATLAB, it is computed that:

```
O = obsv(A_int, C_int);
rank(O)
```

If $\text{rank}(\mathcal{O}) = n = 4$, the system is **fully observable**, and it is possible to construct a full-order **Kalman filter** (optimal observer):

$$\dot{\hat{x}}_{\text{int}} = A_{\text{int}}\hat{x}_{\text{int}} + B_{1,\text{int}}\tilde{u} + K_f(y - C_{\text{int}}\hat{x}_{\text{int}}) \tag{1.59}$$

where K_f is the **Kalman gain**, computed to optimally minimize the estimation error covariance under the assumption of white Gaussian process and

measurement noise. The Kalman gain is derived from the steady-state solution of the continuous-time algebraic Riccati equation:

$$A_{\text{int}}P + PA_{\text{int}}^T - PC_{\text{int}}^T R^{-1} C_{\text{int}} P + Q = 0 \tag{1.60}$$

$$K_f = PC_{\text{int}}^T R^{-1} \tag{1.61}$$

Here:

- Q is the covariance matrix of the process noise,
- R is the covariance matrix of the measurement noise,
- P is the steady-state error covariance matrix.

By solving the Riccati equation with appropriately chosen Q and R, the filter gain K_f ensures that the estimation error converges in a statistically optimal sense, even in the presence of measurement and process disturbances.

Conclusion:
The MATLAB analysis confirms that $\text{rank}(\mathcal{O}) = 4$, which equals the number of internal states. Therefore, the pair $(A_{\text{int}}, C_{\text{int}})$ is **fully observable**, and a Kalman filter can be designed. This guarantees that despite partial measurements, the entire internal state vector $\tilde{x}_{\text{int}}$ can be optimally reconstructed for control and estimation purposes.

This observability ensures that despite partial measurements, the entire controllable state can be reconstructed and regulated accordingly.

Chapter 2

Application

2.1 Simulator description

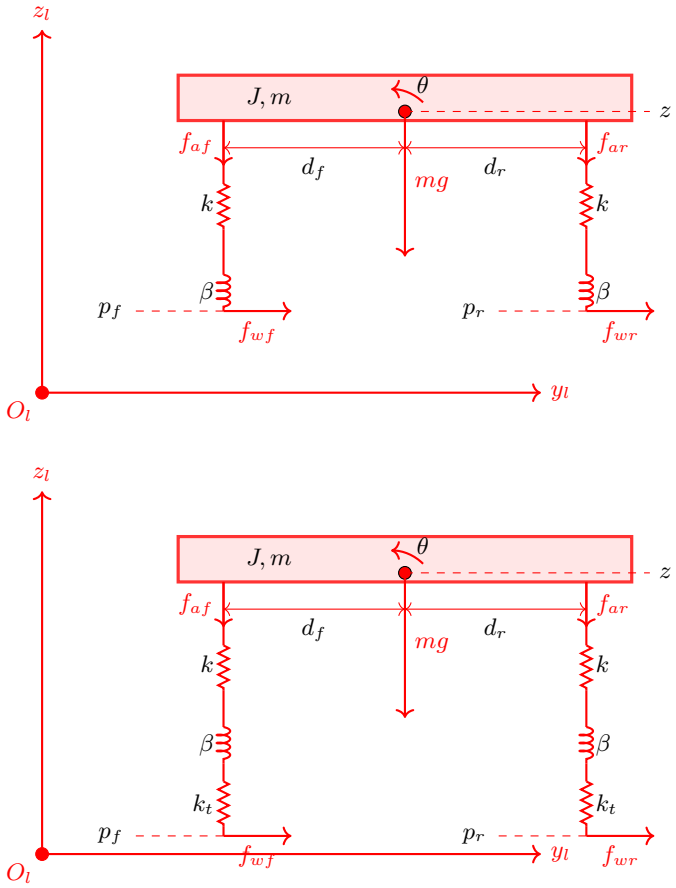

todo: finire sto disegno

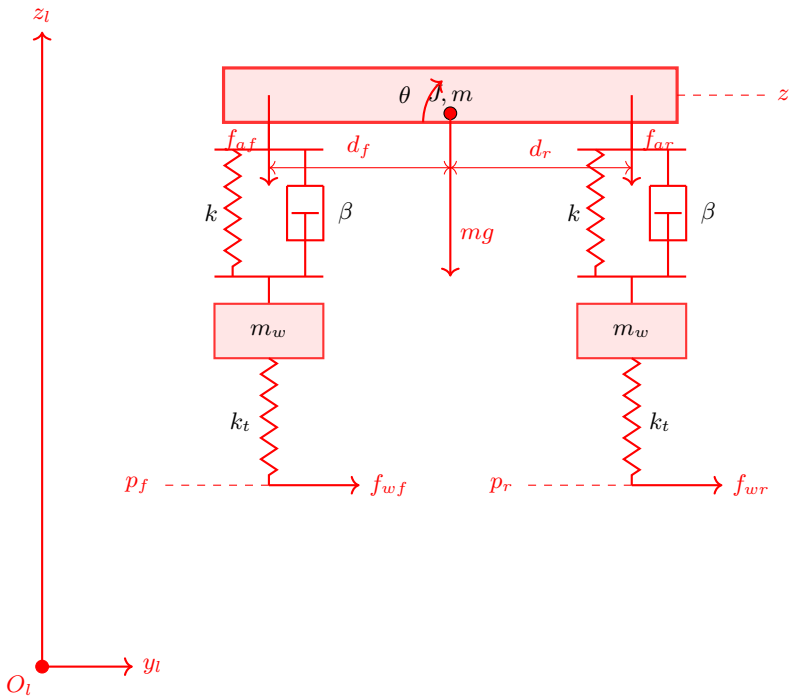

Copy and past the Simulink block scheme and describe what each block does. Describe the set-up MATLAB file, where and how to change the parameters of the simulations. Remember to include also the sensor noises and realistic external disturbances.

2.2 Simulation results

Describe the simulation scenario: initial conditions, purpose of the simulation. Describe the results: are the results coherent with the expectation? If not why? Investigate the tuning: how the performance are affected by the selection of the parameters at disposal of the designer?

Chapter 3

Conclusions and further investigation

Recap the main results obtained in the project and highlight eventual further investigation directions alogn which the performance could be improved.

Bibliography

List the papers/books cited.

Appendix

Use appendices to add technical parts which are instrumental for the completeness of the manuscript but are too heavy to be included inside the main text. Basically, appendices are exploited to let the main text cleaner and smoother. As example, the complete MATLAB listings can be reported in appendix.